HHS Public Access

Author manuscript

Q J Nucl Med Mol Imaging. Author manuscript; available in PMC 2019 May 02.

Published in final edited form as:

Q J Nucl Med Mol Imaging. 2008 June ; 52(2): 134–139.

Sustainable production of orphan radionuclides at Wisconsin

R. J. NICKLES[1], **M. A. AVILA-RODRIGUEZ**[1], **J. A. NYE**[2], **E. N. HOUSER**[1], **R. G. SELWYN**[1], **M. J. SCHUELLER**[3], **B. T. CHRISTIAN**[1], and **M. JENSEN**[1,4]

[1]Medical Physics Department University of Wisconsin, Madison, WI, USA

[2]Emory University, Atlanta, GA, USA

[3]Brookhaven National Laboratory, Upton, NY, USA

[4]Hevesy Laboratory, Risoe Natational Lab Technical University of Denmark, Roskilde, Denmark

Abstract

Over a hundred proton-induced reactions have been studied at the University of Wisconsin Medical Physics department since the installation of the first CTI RDS 112 in 1985. The focus has been to measure thick target yields at 11 MeV, in an effort to concentrate on the practical production of positron emitting radionuclides that have favorable decay characteristics, high yields and the potential for labeling pivotal biological tracers. This review covers our recent advances to scale-up the production of the heavy halogens and transition metals as feed-stock for non-conventional PET tracers that are currently attracting increased attention in oncology.

Keywords

Radionuclides; Radiopharmaceuticals; Tomography; emission computed

Positron emission tomography (PET) extends the promise of quantitatively imaging trace levels of pivotal bio-compounds, ranging in simplicity from oxygen to potent neural ligands implicated in the most subtle of disease states. This broad brush is possible because of the chemical versatility of the “conventional” radionuclides that act as feedstock in the synthesis of the PET radiopharmaceutical. The quartet, ^{18}F, ^{11}C, ^{13}N and ^{15}O, have long been regarded as the major building blocks, listed in descending order of half lives and, not surprisingly, the number of ligands that have been successfully developed.

This simplistic view overlooks the hundreds of other positron emitting radionuclides that span the proton-rich terraces above the valley of β-stability, from ^{10}C to the rare earths. Viewed from this northwest landscape, an increasing number of candidates emerge with β^+ branching ratios, half lives and attractive chemistry that warrant serious re-consideration to label biological tracers, even if bearing the sobriquet of “non-conventional” or “orphan” radionuclides. In particular, the heavier halogens ^{34m}Cl, ^{76}Br and ^{124}I, as well as a number

Address reprint requests to: Dr. R. J. Nickles, School of Medicine and Public Health, Department of Medical Physics, 1530 Medical Sciences Center, 1300 University Ave, Madison, WI 53706, USA. rnickles@wisc.edu.

of transition metals, are poised to fill a significant role in labeling diagnostic agents directed toward the study of neoplastic disease.

Resources

Accelerators

The “heavy steel” of any PET site is the accelerator, which at the University of Wisconsin has employed in sequence: an EN tandem (installed in 1957; 12 MeV protons and deuterons; 10 μA; UW Physics Department), the first CTI RDS 112 (1985; 11 MeV protons; 50 μA; UW Medical Physics Department) and, most recently, an NEC 9SDH-2 tandem (1999; 6 MeV protons and deuterons; 120 μA; UW Keck Neuroscience Laboratory). All of three accelerators are bunkered with full access to targets on multiple beam-lines that allow target development and telemetry in unrestrained geometry. This paper will discuss work done primarily on the 11 MeV proton cyclotron over the past two decades, investigating the yields and applications of the positron emitters between $6 \leq Z \leq 53$.

Targets

Liquid targets include: a high-pressure niobium gridded target[1] for [^{18}F]fluoride; a flow-through [^{13}N]ammonia target;[2] and a He-sparged cell for the steady state production of the noble gas pair ^{79}Kr/^{81m}Kr from the irradiation of bromoform. Various gas targets produce $^{18}F_2$ from $^{18}O_2$ by the “two-shoot” technique,[3] and a number of aluminum, stainless and niobium flow-through targets for the production of $^{14}O_2$, $^{15}O_2$ and $^{11}CH_4$.

About a dozen specialty targets have been developed to irradiate solid materials, with the greatest challenge being the production of $^{10}CO_2$ for steady state inhalation to image regional blood flow. The absence of recirculation with $^{10}CO_2$ ($t_{1/2}$=19 s) is evident in Figure 1. This collage shows the equilibrium distribution of activity during constant inhalation of the four radio-isotopic forms of carbon dioxide, cognizant of the fact that label exchange results in the immediate transfer of labeled oxygen to water. While $^{10}CO_2$ has found modest clinical appeal,[4] its production demands serious attention to the irradiation of helium-swept, incandescent $^{10}B_2{}^{18}O_3$ targets (Figure 2). At the extreme limit, a vertical switching magnet was constructed to focus a downward-directed beam onto the most corrosive of the molten targets, constrained by gravity[5] from burning their way into the cyclotron interior. These hard-won lessons, learned in the crucible of $^{10}CO_2$ production, bear fruit in the more relaxed bombardment conditions leading to ^{124}I and the transition metals.

Telemetry

To irradiate a costly target at kW power levels without constantly watching the immediate consequences is an invitation to disaster. The visible signature of a nuclear reaction is the outgoing, penetrating radiation, namely neutrons and gammas. The prompt γ spectrum is dominated by inelastic scattering during irradiation, which at least confirms that the correct target is receiving beam. Conversely, for target materials electroplated onto gold blanks, the sudden appearance of the signature 497 keV γ from ^{197}Au(p,p’) is a warning of a thin, or flaked target. The concurrent neutron flux, absorbed in the bunker walls, gives rise to an overwhelming γ background, necessitating massive collimation of the γ detector to restrict

the solid angle to the target only. Finally, the γ spectrum is further confounded by neutron activation of the γ detector itself. A germanium detector would only last minutes in the fast neutron flux, while NaI(Tl) quickly activates with ^{24}Na (isomeric and ground state) and ^{128}I. Bismuth germanate and yttrium aluminum perovskite do not activate, but energy resolution is sacrificed. Both LSO and the lanthanum trihalides (LaX_3 (Ce); X=Cl, Br) have excellent energy resolution and speed needed in the high γ flux. The bromide is favored for energy resolution, but suffers from modest neutron activation to ^{80}Br that requires correction of the γ signal time course. After a protracted search, two γ detectors are employed. The first is a 4×4 cm $LaBr_3$ detector, laser aligned within its 200 kg lead collimator at 5 m to view the 1 μ-steradian target field (Eγ>1 MeV). The second is a simple plastic scintillator mounted on a photomultiplier tube operated in the current mode. By consistently monitoring these γ signals, a wide variety of target problems can be diagnosed and remedied.

The neutron flux is sensed with a BF_3 “long counter” at several meters from the target, chosen for its excellent n/γ discrimination. Uranium-235 fission counters have similar favorable γ insensitivity, but seem to have an operational lifetime only of the order of a year. The geometry and 10^{-4} sensitivity of the long counter result in 10^4 cps counting rates at realistic bombardment conditions, making the neutron flux the primary signature of the irradiation progress. Crowbars, vapor voids and drifting beam over target thickness inhomogeneities are all immediately apparent in a glance at the display of the neutron and gamma flux, logged at 10-s intervals. Furthermore, the zero background makes the neutron counting rate n the perfect input signal for the leaky integration of the difference equation $\Delta N/\Delta t = n-\lambda N$,, describing the incremental buildup of the product N, proportional to the neutron counting rate less the decay. Gammas, neutrons and the leaky integrator are displayed on the Labview interface control page that forms the new operating system for our legacy RDS 112.[6]

The raw neutron and γ flux is shown in Figure 3, normalized to 1 μA of 11 MeV protons on such thick targets as elemental ^{197}Au, $^{14}N_2$, ^{6l}Ni, ^{89}Y, ^{64}Ni, ^{nat}Kr, and $^{18}O_2$. The advantage of choosing a target backing substrate and slit material from high-Z materials (Au, Ta) is obvious in terms of reducing neutron backgrounds, that would otherwise obscure the desired target signal. Nonetheless, the ratio of the neutron flux from irradiating highly enriched [^{18}O]-water to natural water is only a factor of three. Given that 11 MeV protons on [^{16}O]-water cannot result in neutrons, the failure to observe a factor of 500 expected from the natural abundances alerts us to the neutron background from beam lost on slits, foils and other internal structures.

Methodology

Five unconventional PET radionuclides with longer half-lives have captured the interest of researchers at Wisconsin (Table I), along with the reaction, half-life, target chosen, measured end-of-saturated-bombardment yield extrapolated to a thick target of the stated target compound, at 100% enrichment, a representative application and local references.

Copper isotopes

The relative dosimetry, logistics and economics of the various copper isotopes have been well described in the literature,[16] with 4 isotopes, ^{60}Cu, ^{61}Cu, ^{62}Cu and ^{64}Cu contending for clinical applications. Copper-64, with its 12.7 h half-life stands alone for labeling ligands with protracted blood clearance, or for national distribution by commercial carriers. This same lifetime confounds its use in sequential patient studies, or in the case of veterinary patients, impeding the immediate release of the pet to its owner following the study. Copper-61 has more favorable dosimetry and positron imaging characteristics, and has found a preclinical role in the imaging of tumor hypoxia responding to therapy. Our experience shows that more than an hour is needed for the tumor distribution of Cu-ATSM to stabilize, ruling out the shorter-lived ^{60}Cu or generator-accessible ^{62}Cu.

The close race between ^{61}Cu and ^{64}Cu to label Cu-ATSM hinges on a second tier of considerations: commercial availability, flexibility of patient scheduling, cyclotron loading, and coupling to fixed distribution schedules. If these considerations dictate that ^{61}Cu-ATSM is favored, then three entrance channels present themselves at our site: ^{61}Ni(p,n)^{61}Cu on enriched ^{61}Ni, ^{64}Zn(p,α)^{61}Cu or ^{60}Ni(d,n)^{61}Cu at 6 MeV deuteron energy on the Keck Lab tandem, with yields in the ratio of 100:5:4.

The target preparation of both the enriched nickel targets are identical, and both tightened by the $17/mg cost of the enriched elemental materials. The metals are electro-plated[7] onto gold discs (99.999%), irradiated, digested, and separated as the chloro-adducts. Nickel elutes in 6N HCl, Co-isotopes in 4N HCl and Cu-isotopes in 0.1N HCl. The nickel is recycled with 95±2% mass recovery, and the copper isotopes are collected for labeling and distribution. TETA-titration shows that $^{64}CuCl_2$ has a specific activity of the order of 19 Ci/μMole, approaching 10% of the carrier-free level. Over the past 2 years, our 20 Ci production has been shared with colleagues at other institutions, with 10 Ci leaving our dock.

Finally, in the case of microspheres for selective internal radiation therapy (SIRT), one of the authors (R. G. S.) has developed a technique to employ ^{64}Cu-labeling, which allowing quantitative dosimetry to the intra-arterial administration of co-injected ^{90}Y-SIR-spheres™ for the treatment of hepatic carcinoma.

Yttrium and zirconium isotopes

The mushrooming application of SIRT, based both on capillary-occlusive ^{90}Y-labeled microspheres and targeted large molecules, demands that PET bring its quantitative, non-invasive potential to bear on the task of imaging the spatial heterogeneity of the treatment. While considered a pure β- emitter, ^{90}Y actually has a 32 ppm positron branch from the E_0 decay of the first excited state of ^{90}Zr,[17] permitting a crude PET imaging through the overwhelming bremsstrahlung. Far better is to co-inject the surrogate ^{86}Y-agent, or if need be, ^{89}Zr-agent with a matching half-life, if the different oxidation states do not seriously affect the chelation.

Early attempts to irradiate metallic strontium targets at high power led to serious problems with target materials and long-lived yttrium products sputtered into the cyclotron interior. The carbonates and oxides of strontium allow 10–20 μ-amp currents if careful attention is

paid to removal of beam power with both water cooling below and turbulent helium flow over the of the beam strike on the target surface.[9] Separation of the ^{86}Y from the alkaline $^{86}Sr^{2+}$ digest makes use of the remarkable affinity of the yttrium hydroxide to filter paper.[18, 19]

The production of ^{89}Zr has the advantage of starting from the naturally occurring ^{89}Y target material, obviating the need for any target reclamation. Straightforward dissolution and ion exchange chromatography suffices to separate Y^{3+} from $^{89}Zr^{4+}$, as shown by X-ray fluorescence[20] and ICP-MS. While both ^{86}Y and ^{89}Zr present additional gammas, ^{89}Zr is favored because its 909 keV γ is delayed by seconds in its isomeric decay, falling far outside the coincidence window in PET imaging.

Iodine-124

Chemists love iodine isotopes, with their labeling versatility under gentle conditions. Iodine-124, once considered a noxious contaminant of ^{123}I from the irradiation of tellurium targets, is now embraced as the poster child of PET for peptide and protein labeling. Alpha irradiation of natural antimony would provide ^{124}I for animal studies, albeit contaminated with ^{126}I, but few cyclotrons with good α beams still remain. The proton irradiation of ^{124}Te as a TeO_2/Al_2O_3 glass at shallow beam incidence is widely used,[21, 22] but is beam-limited by the volatility of both the tellurium and iodine. The binary compound Al_2Te_3 has both a higher melting point and a greater effective fraction of tellurium than other candidates, and can be made from the elements with an exothermic reaction under argon with an enthalpy of formation of 267 kJ/mole. With ^{124}Te, the black glassy aluminum telluride[14, 23] in a target fixture similar to Figure 2 permits beam currents up to 20 μA at 11 MeV, resulting in 173 μCi/μA-hr. Dry distillation at 910 °C in a gentle steam of dry air deposits the ^{124}I downstream on a cooled platinum wire, from which it can be quantitatively harvested in weak base. A commercial system is under development (Comecer SpA, Castel Bolgnese, Ravenna, Italy).

Results and conclusions

The decision to scale up the local production of the five radioisotopes in Table I came about when the expected benefits outweighed the costs. At the tipping point, the benefits are potential, belonging to the realm of the future, while the costs are real and immediate. In particular, the concept of opportunity cost, the value of an opportunity forgone, dominates both sides of the balance: to wait for some commercial supplier to provide ^{64}Cu on a nationwide level means forgoing, delaying research opportunities that need it now. On the other hand, to commit the resources for enriched ^{64}Ni, gold blanks, Ultrex reagents and large blocks of beam time means that other cyclotron projects will be left undone. Opportunity cost accounting is notoriously fickle, but a reasonable value for beam time can be estimated by its worth in the likely alternate enterprise of FDG production, easily justifying a $300/h figure. The case for pursuing local ^{64}Cu production is the most obvious, given the mushrooming interest in labeling a wide variety of large molecules, a half-life well matched to national distribution of the excess, and the large cross section even at 11 MeV that permits Curie levels to be made during the off hours.

The regular production of ^{64}Cu starts each Monday morning, with 5 local research groups able to count on tens of millicuries on Monday, a few millicuries on Tuesday and microcuries throughout the rest of the week. MicroPET (P4 and Inveon) sensitivities are so great that targeted tracers bearing tens of microcries suffice in the nude mouse models. Generally half of our ^{64}Cu production is shipped by FedEx overnight priority to several collegial institutions, which provide us with valuable feedback as we improve our specific activity. This ratio of ^{64}Cu to cold copper has now reached almost 1/10th of the carrier free level shown by TETA-titration, and our distant colleagues are reporting much improved labeling of their nano-mole levels of ligand.

The production of non-conventional radionuclides on the UW RDS 112 started out as a shotgun reconnaissance of the proton-rich side of the valley of β stability, crudely determining what was feasible with 11 MeV protons before succumbing to the Coulomb barrier in the rare earths. This search matured into a fertile field for a half dozen PhD dissertations, each improving and extending the reach of our legacy cyclotron. Now more than a simple survival strategy, the production of these orphan isotopes opens the doorway to a sustainable future: a seasoned cyclotron with a new brain, with the will and capacity to provide a significant fraction of the national needs.

Acknowledgments

Funding.—This study was supported by grants DOE DE-FG01-01NE23052 and NIH/NCI 5 T32 CA09206.

References

1. Nye JA, Avila-Rodriguez MA, Nickles RJ. A grid-mounted niobium body target for the production of reactive [^{18}F]-fluoride. Appl Radiat Isot 2006;64:536–9. [PubMed: 16368243]
2. Nickles RJ, Martin CC, Christian BT, Stone CK. Flow-through trapping to soften N-13 ammonia logistics. J Nucl Med 1992;33:931
3. Nickles RJ. Daube ME. Ruth TJ. An $^{18}O_2$ target for the production of, $^{18}F_2$. Int J Appl Radiat Isot 1984;35:117.
4. Law I, Jensen M, Holm S, Nickles RJ, Paulson OB. Using $^{10}CO_2$ for single subject characterization of the stimulus frequency dependence in visual cortex: a novel positron emission tomography tracer for human brain mapping. J Cereb Blood Flow Metab 2001;21:1003–12. [PubMed: 11487736]
5. Jensen M, Wolber G, Nickles RJ. Runz A. Gravity can offer help: stable production of c-10 by bombarding a molten sea of boron oxide with a vertical proton beam. 9th International Workshop on Targetry and Target Chemistry, C5 Turku, Finland: May 2002p.23–25.
6. Smith EN, Vandehey NT. Murali D, Davidson RJ. Nickles RJ, Christian BT. Updating computer control for an RDS-112 and a CPCU. J Labelled Comp Radiopharm 2007; 50: S1, P020.
7. Avila-Rodriguez MA. Low energy cyclotron production of multivalent transition metals for PET imaging and therapy. UW Medical Physics PhD Dissertation Madison, WI: 2007.
8. Avila-Rodriguez MA, Nye JA, Nickles RJ. Simultaneous production of high specific activity Cu-64 and Co-61 with 11.4 MeV protons on enriched Ni-64 nuclei. Appl Radiat Isot. In press, 2007.
9. Avila-Rodriguez MA, Nye JA, Nickles RJ. Production and separation of non-carrier-added Y-86 from enriched Sr-86 nuclei. Appl Radiat Isot. In press 2007.
10. Avila-Rodriguez MA, Selwyn RG, Converse AK, Nickles RJ. Y-86 and Zr-89 as PET imaging surrogates of Y-90: a comparative study. AIP Conference Proceedings 2006;845:45–7.
11. Nickles RJ, Roberts AD, Nye JA, Converse AK, Barnhart TE, Avila-Rodriguez MA et al. Assaying and PET imaging of Ytrrium-90: l>>34ppm>0. IEEE Nuclear Science Symposium Conference Record 2004;6:3412–24.

12. Avila-Rodriguez MA, Selwyn RG, Hampel JA, Thomadsen BR, Dejesus OT, Converse AK et al. Positron-emitting resin microspheres as surrogates of ^{90}Y SIR-Spheres: a radiolabeling and stability study. Nucl Med Biol 2007;34:585–90. [PubMed: 17591559]

13. De Jesus OT, Nickles RJ. Production and purification of Zr-89: a potential PET antibody label. Int J Rad Appl Instrum [A] 1990;41:789–90.

14. Nye JA, Avila-Rodriguez MA, Nickles RJ. A new binary compound for the production of I–124 *via* the ^{124}Te(p,n)^{124}I reaction. Appl Radiat Isot 2007;65:407–12. [PubMed: 17174098]

15. Nye JA, Avila-Rodriguez MA, Nickles RJ. Production of [^{124}I]-iodine on an 11 MeV cyclotron. Radiochimica Acta 2006;94:213–6.

16. McCarthy DW, Bass LA, Cutler PD, Shefer RE, Klinkowstein RE, Herrero P et al. High purity production and potential applications of Cu-60 and 61. Nucl Med Biol 1999;26:351–8. [PubMed: 10382836]

17. Selwyn RG, Nickles RJ, Thomadsen BR, DeWerd LA, Micka JA. A new internal pair production branching ratio of Y-90: The development of a non-destructive assay for Y-90 and Sr-90. 2007. Appl Rad Isotopes 2007;65:318–27.

18. Friedlander J, Kennedy JW, Macias ES, Miller JM. Nuclear and radiochemistry, 3rd ed New York: John Wiley and Sons; 1981p.296.

19. Avila-Rodriguez MA, Murali D, Nickles RJ. A rapid and efficient method for the separation of non-carrier-added ^{86}Y from strontium-based targets. J Nucl Med 2007;48:320P.

20. Nickles RJ, Avila-Rodriguez MA, Houser EN, Selwyn RG. Finding a Niche for XRFS in the PET radiochemistry lab. J Labelled Comp Radiopharm 2007;50:S1.

21. Finn RD, Sheh Y, Bui V, Larson SM, Schlyer D. Refinements with targetry to overcome accelerator energy constraints. Nucl Instrum Meth Phys Res Sect B 1995;99:814–6.

22. Qaim SM, Gigb A, Bastian T, El-Azoney KM, Blessing G, Spellerberg S et al. Some optimization studies relevant to the production of high purity ^{124}I and ^{120g}I at a small sized cyclotron. Appl Radiat Isot 2003;58:69–78. [PubMed: 12485666]

23. US Patent P04326US, Systems and methods for the cyclotron production of Iodine-124, JA Nye and RJ Nickles (given to WARF), 2006.

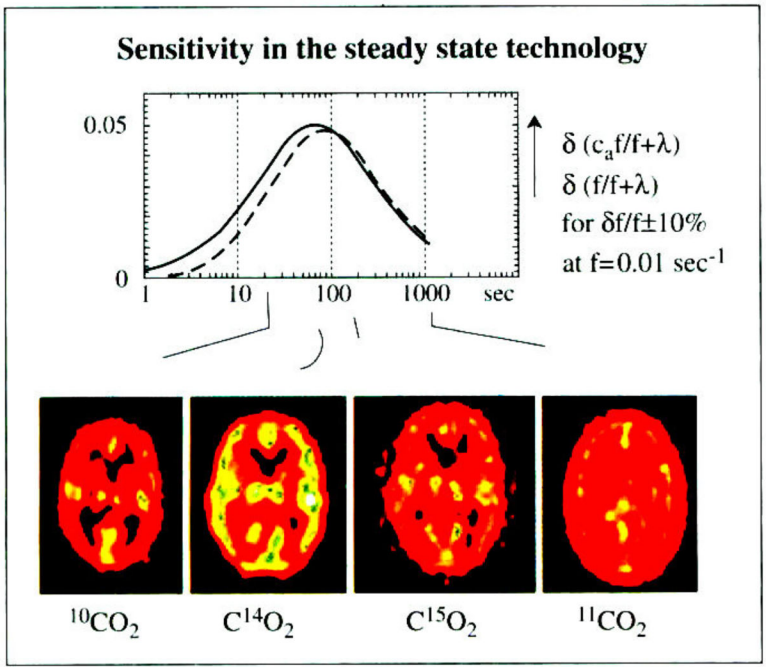

Figure 1.—.

The sensitivity of the steady state technique for the measurement of regional blood flow is determined between the "impedance matching" of mass specific flow f (mL/s/gram of tissue = s^{-1}) to the mean decay rate $\lambda=\ln 2/t_{1/2}$. The optimal half life is 71 s for grey matter flow, where a 10% variation in f would result in a 5% variation in the equilibrium activity, slightly displaced to the right when accounting for the lung-to-brain arterial delay $c_a(t)$. The PET steady state flow images of the normal subjects reflect the increased contrast at the shorter lifetime CO_2 tracers.

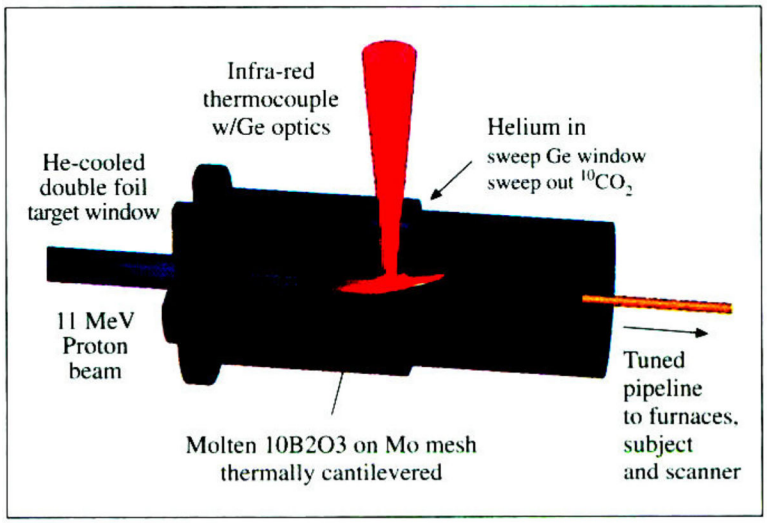

Figure 2.—.

The $^{10}B_2O_3$ target with He-swept $^{10}CO_2$ represents the extreme case of handling molten materials in the beam strike. Adjusting the helium flow, beam and thermal cantilevering determines the target temperature, which optimizes the diffusion and transport of the 19-s product.

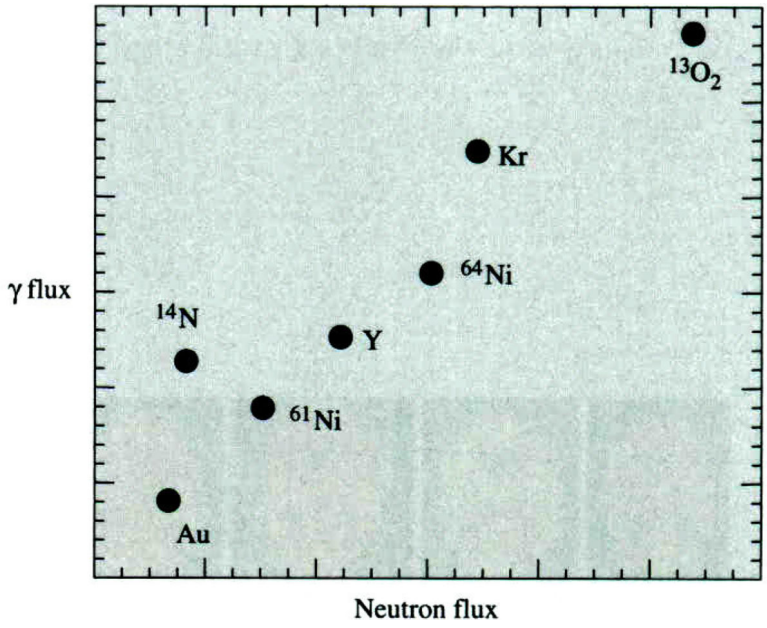

Figure 3.—.

A linear plot (in arbitrary units) of the relative γ to neutron flux rates per unit beam current, demonstrating the "signature" of various thick target substrates under 11 MeV proton irradiation. Elements without superscripts denote the naturally occurring abundance.

Table I.—

Five unconventional positron emission tomography radionuclides with longer half-lives.

Reaction	$t_{1/2}$	Target	Yield (mCi/μA)	Application	Reference
$^{61}Ni(p,n)^{61}Cu$	3.4 h	^{61}Ni on Au	105	Preclinical Cu-ATSM	7
$^{64}Ni(p,n)^{64}Cu$	12.7 h	^{64}Ni on Au	181	Large molecules	8
$^{86}Sr(p,n)^{86}Y$	14.7 h	$^{86}SrCO^{3}$	27	PET surrogate for ^{90}Y	9–12
$^{nat}Y(p,n)^{89}Zr$	78 h	^{nat}Y-foil	100	Peptide labeling	13
$^{124}Te(p,n)^{124}I$	4.2 d	$Al_2{}^{124}Te_3$	33	Many	14, 15